공학석사학위논문

자연 유래 갈릭산 유도체로 가교된 고체상 고분자 전해질의 제조 및 전고체 리튬황전지로의 응용

Solid Polymer Electrolytes Based on Polysiloxane Crosslinked by Modified Natural Gallic Acid for All-Solid-State Lithium-Sulfur Battery Applications

2017년 2월

서울대학교 대학원

화학생물공학부

김 루 시 아

자연 유래 갈릭산 유도체로 가교된 고체상 고분자 전해질의 제조 및 전고체 리튬황전지로의 응용

Solid Polymer Electrolytes Based on Polysiloxane Crosslinked by Modified Natural Gallic Acid for All-Solid-State Lithium-Sulfur Battery Applications

지도교수 이 종 찬

이 논문을 공학석사 학위논문으로 제출함.

2017년 2월

서울대학교 대학원

화학생물공학부

김 루 시 아

김루시아의 석사학위논문을 인준함.

2017년 2월

위 원 장 _____(印)

부위원장 _____ (印)

위　　원 _____(印)

Abstract

Solid Polymer Electrolytes Based on Polysiloxane Crosslinked by Modified Natural Gallic Acid for All-Solid-State Lithium-Sulfur Battery Applications

Lucia Kim

Polymer Chemistry

Department of Chemical & Biological Engineering

Seoul National University

Solid polymer electrolytes (SPEs) based on polysiloxane having ion-conducting poly(ethylene oxide) (PEO) groups crosslinked with modified gallic acid from natural resources were prepared by thiol-ene click reaction for all-solid-state lithium-sulfur batteries. The effects of crosslinking density on thermal/mechanical and electrochemical properties were systematically studied. SPEs were found to be thermally and mechanically stable even at elevated temperature due to formation of stable crosslinked polymer network by modified gallic acid crosslinker. Furthermore, SPE based on 80 mol% of PEO group and 20 mol% of modified gallic acid crosslinker exhibited high ionic conductivity comparable to that of waxy polymer electrolyte having only the PEO group without crosslinking.

All-solid-state lithium-sulfur battery was fabricated by preparing SPE integrated sulfur cathode and it is expected that SPE can act as mechanical and chemical barrier against dissolution of lithium polysulfides, resulting in excellent cycle performance at high temperature.

Keywords: lithium-sulfur battery, all-solid-state lithium metal battery, solid polymer electrolyte, gallic acid, thiol-ene click chemistry

Student Number: 2015-21041

List of Schemes

List of Figures

Figure 9. Linear sweep voltammogram A-BPTP80 at 60 ^{o}C with a scan rate of 1 mV/s.

Figure 10. Interfacial resistances of symmetric lithium cell containing A-BPTP80 stored under open-circuit condition at 60 ^{o}C as a function of storage time.

List of Contents

1. Introduction

Lithium-sulfur batteries have attracted a great deal of attention as the next-generation of battery system due to their high energy densities compared to those of conventional lithium-ion batteries.[1, 2] Since the sulfur has a wide range of oxidation states, it can generate high capacity as cathode active materials especially when it was coupled with lithium metal anode.[3] Furthermore, sulfur is very cheap, nontoxic, and abundant in the earth's crust which realizes low-cost and green battery systems.[4] However, current lithium–sulfur batteries have faced fundamental challenges originated from insulating property of elemental sulfur and lithium sulfides, continuous dissolution of lithium polysulfides into the liquid electrolytes, and formation and growth of lithium dendrites.[1-4] To resolve these issues, various approaches such as encapsulation of sulfur by highly-conductive carbon materials[5-8] and conducting polymers,[9-11] and modification/fabrication of separator[12-15] have been suggested. Still, those efforts cannot fully control the complicated problems occurred in both sulfur cathode and lithium metal anode.

Development of all-solid-state lithium-sulfur battery system can give promising solutions to these challenges, because solid polymer electrolyte (SPE) acts as chemical and mechanical barriers against the dissolution of lithium polysulfides.[16] Furthermore, SPEs effectively suppress the formation and growth of lithium dendrites.[17, 18] Still, low ionic conductivity and insufficient mechanical stability of the SPEs based on ion-conducting poly(ethylene oxide) (PEO) derivatives have to be resolved.[16, 19] The low ionic conductivities of the SPEs can be increased by grafting low molecular weight PEO side chains or introducing of plasticizers, while this can also decrease the mechanical strength.[20-23] The mechanical stability of the SPEs can be increased by using crosslinkers or filler materials.[24-28] Among them, ion-conducting polymer materials having low molecular weight PEO side chains and crosslinkable moieties are promising candidates for the high-performance SPEs because they can exhibit high ionic conductivity as well as sufficient mechanical strength.[26-28] However, commercially available crosslinkers are usually derived from petroleum sources which have resource limitation problem in the near future. Natural plant-derived phenolic acids have been used as functional monomers or

crosslinkers for various purposes such as coatings and adhesives applications because they have rigid aromatic rings that can provide mechanical strength.[29-32] Moreover, further modification of phenolic acids should be easy because they have hydroxyl and/or carboxyl groups.[33] Various chemical and physical properties of resulting polymers having modified phenolic acids can be readily tuned by modifying the functional groups of phenolic acids.[34] Among a variety of phenolic acids, gallic acid having a rigid benzene ring, three phenol groups, and one carboxylic group is ubiquitously found in many plants such as gallnuts, sumac, witch hazel, and tea leaves, and has been widely used in various kinds of industry.[35, 36] However, such modifications and applications of phenolic acids to be used as monomers or crosslinkers for the SPEs have not been reported many times.

Herein, SPEs based on polysiloxane having ion-conducting PEO group crosslinked with modified phenolic acid, gallic acid, by thiol-ene click chemistry were prepared and applied to high-temperature all-solid-state lithium-sulfur batteries (Scheme 1). The effects of crosslinking density of the SPEs on various physical and electrochemical properties were systematically studied. It was found that our SPEs

Scheme 1 Development of all-solid-state lithium-sulfur battery containing solid polymer electrolyte (SPE) based on natural phenolic acid, gallic acid.

exhibit high ionic conductivity even comparable to polysiloxane having only PEO group with a wax state and good mechanical stability especially at elevated temperature.

2. Experimental

2.1.Materials

(3-Mercaptopropyl)methyldimethoxysilane, (3-mercaptopropyl)trimethoxysilane, and 3,4,5-trihydroxybenzoic acid (gallic acid) were purchased from Alfa Aesar and used as received. Poly(ethylene glycol) methyl ether (average M_n = 400 g mol^{-1}), , allyl bromide, and 2,2-dimethoxy-2-phenylacetophenone) were purchased from Aldrich and used as received. Lithium bis(trifluoromethane sulfonyl)imide (LiTFSI, >98%, TCI) was dried under high vacuum at 130 ^{o}C for 24 h and subsequently placed in an argon filled glove box. All other reagents and solvents were obtained from reliable commercial sources and used as received.

2.2.Synthesis of branched polysiloxane having thiol group (BPT)

Branched polysiloxane having thiol group (BPT) was synthesized by acid-catalyzed hydrolysis and condensation reaction (Scheme 2(a)). Hydrochloric acid (10.4 g, 0.104 mol) was dissolved in a mixed solvent (water-ethanol mixture) and resultant solution was added to a 100 mL of one-neck round bottomed flask equipped with a magnetic stirring bar. (3-Mercaptopropyl)methyldimethoxysilane (3.6 g, 0.02 mol) and (3-mercaptopropyl)trimethoxysilane (4.0 g, 0.02 mol) were added to the solution and then heated at 50 ^{o}C for 3 h in an oil bath under nitrogen atmosphere. The crude product was distillated at 80 ^{o}C under vacuum to remove the solvent. Excessive monomers were removed by precipitation of the crude solution in distilled water. After being dried under vacuum at room temperature for 24 h, viscous and transparent oil was obtained with 67 % yield. For the convenience, branched polysiloxane having thiol group is abbreviated as BPT. ^{1}H NMR [300 MHz, $CDCl_3$, δ (ppm), TMS ref] of BPT: 2.55 (Si-CH_2-CH_2-C*H*$_2$-SH), 1.67 (Si-CH_2-C*H*$_2$-CH_2-SH), 1.35 (-S*H*), 0.62 (Si-C*H*$_2$-CH_2-CH_2-SH), 0.12 (Si-C*H*$_3$). ^{29}Si

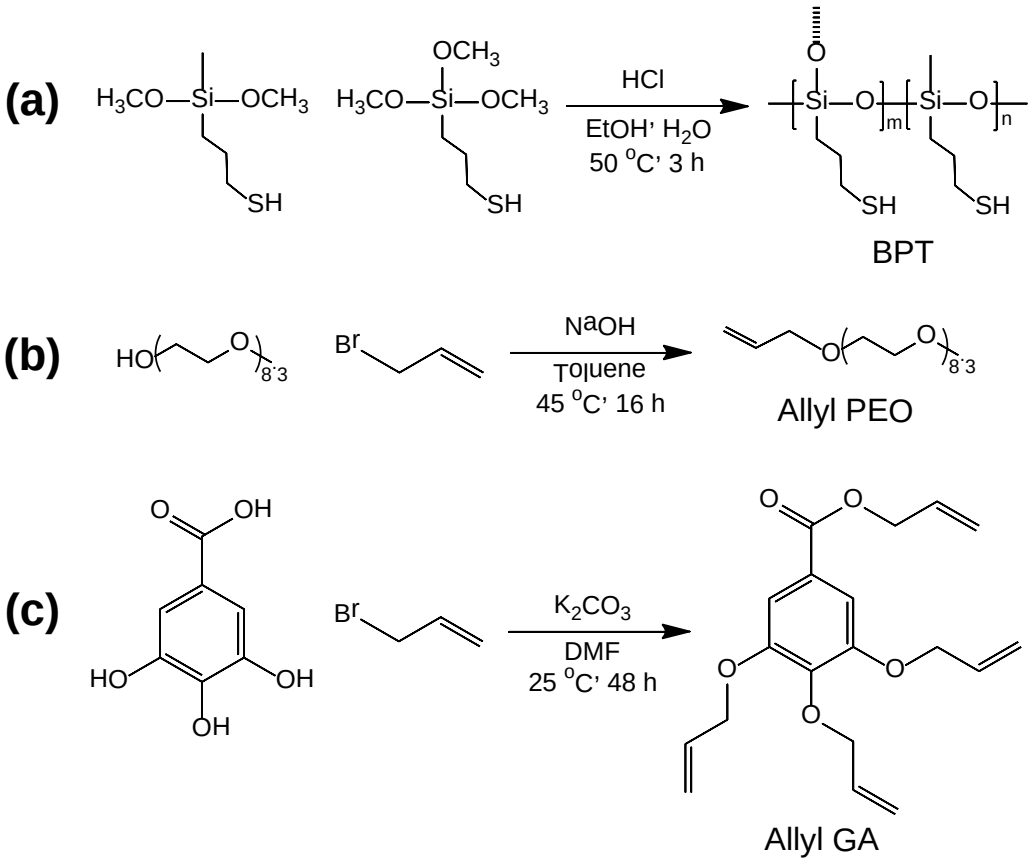

Scheme 2 Synthesis of (a) branched polysiloxane having thiol group (BPT), (b) allyl poly(ethylene oxide) (allyl PEO), and (c) allyl gallic acid (allyl GA).

NMR [400 MHz, $CDCl_3$, δ (ppm), TMS ref] of BPT: -15.8 (D) and -68 (T).

2.3.Synthesis of allyl poly(ethylene oxide) (allyl PEO)

Poly(ethylene glycol) methyl ether (M_w 400) (40 g, 0.10 mol) and allyl bromide (13 g, 0.11mol) were reacted under the presence of sodium hydroxide (4.4 g, 0.11 mol) in distilled toluene at 45 ^oC for 16 h (Scheme 2(b)). The residual solvent was removed under reduced pressure by evaporation. Crude product was dissolved in dichloromethane and extracted with distilled water three times. After being dried under anhydrous magnesium sulfate, transparent liquid was obtained with 92 % yield. For the convenience, allyl poly(ethylene oxide) is abbreviated as allyl PEO. ^{1}H NMR [300 MHz, $CDCl_3$, δ (ppm), TMS ref] of allyl PEO: 5.92 (vinyl, C*H*$_2$), 5.25 (vinyl, C*H*), 4.11 (CH_2=CH-C*H*$_2$-O), 3.57-3.77 (C*H*$_2$-C*H*$_2$-O), 3.38 (C*H*$_3$-O).

2.4.Synthesis of allyl gallic acid (allyl GA)

Gallic acid (1 g, 1 mol) was dissolved in 40mL of anhydrous DMF with potassium carbonate (3.25 g, 4 mol), and the mixture was transferred to a 250 mL round-bottomed flask equipped with a magnetic stirring bar at 25 ^{o}C (Scheme 2(c)). Allyl bromide (2.84 g, 4 mol) was slowly added to the solution by dropwise and the resultant mixture was stirred for 48 h under nitrogen atmosphere. After the reaction, the crude product was dissolved in ethyl acetate and extracted with distilled water three times and the organic layer was collected. After being dried under anhydrous magnesium sulfate, yellow liquid was obtained with 88 % yield. For the convenience, allyl gallic acid is abbreviated as allyl GA. ^{1}H NMR [300 MHz, DMSO-d_6, δ (ppm), TMS ref] of allyl GA: 7.25 (phenyl, C*H*), 5.8~6.1 (vinyl, C*H*), 5.1~5.5 (vinyl, CH_2), 4.5~4.8 (CH_2=CH-CH_2-O).

2.5.Preparation of solid polymer electrolytes (SPEs): A-BPTPs

SPEs were prepared by thiol-ene click reaction under fluorescent lamp irradiation (Scheme 3(a)). SPE containing 80 mol% of PEO group and 20 mol% of allyl GA group was prepared as follows. BPT (0.1 g, 0.85 mmol of thiol group), allyl PEO (0.26 g, 0.67 mmol), allyl GA (0.014 g, 0.042 mmol), LiTFSI (0.113 g, [Li]/[EO] = 0.07), and DMPA (0.01 g, 0.039 mmol) were dissolved in 0.4 mL of distilled THF. The solution was cast onto a glass plate (2.5 × 2.5 cm^2) and the THF solvent was removed under ambient condition. Subsequently, florescent lamp (BT-36DP, 36 W, SUNSEA Co., LTD, Korea) was irradiated to the glass plate for 16 h. The film was peeled from the glass plate and the resultant film was dried under high vacuum condition for a week at 60 ºC prior to further characterization. Other SPEs having different PEO content and crosslinking density were also prepared using the same procedure except the feed ratio of allyl PEO and allyl GA. For the convenience, SPEs crosslinked with allyl GA are abbreviated as A-BPTPs. Especially when the feed mole ratios of allyl PEO to allyl GA were 50:50, 65:35, and 80:20, they were

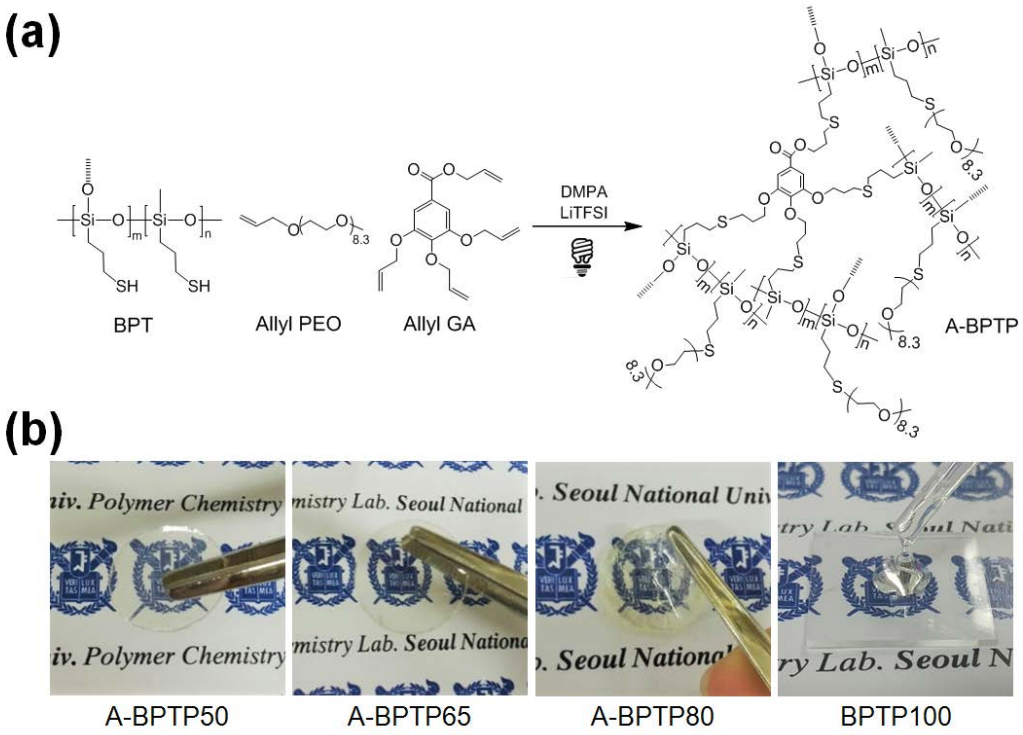

Scheme 3 (a) Preparation of A-BPTPs by thiol-ene click reaction under fluorescent lamp irradiation and (b) free-standing film states of A-BPTPs and wax state of BPTP100, where the number in the abbreviation indicates mol% of allyl PEO.

named as A-BPTP50, A-BPTP65, and A-BPTP80, respectively. And the numbers in the abbreviations represent mol% of allyl PEO group.

2.6.Synthesis of branched polysiloxane having PEO side chains (BPTP100)

BPT (1.0 g, 7.2 mmol of thiol group), allyl PEO (3.62 g, 9.2 mmol), and 2,2-dimethoxy-2-phenylacetophenone (DMPA) (0.09 g, 0.35 mmol) were dissolved in 0.5 mL of distilled THF and stirred for 10 min under irradiation of UV light (OV-11 ultraviolet lamp, 60 Hz, FORCELAMP Co., LTD, Korea). Excessive allyl PEO was removed by precipitation of the crude product in *n*-hexane three times. After being dried under vacuum at room temperature for 24 h, viscous wax was obtained with 95 % yield. For the convenience, branched polysiloxane having PEO side chains is abbreviated as BPTP100, where 100 indicates that 100 mol% of thiol group in BPT is substituted by the allyl PEO, which is confirmed from the ^{1}H NMR result. ^{1}H NMR [300 MHz, $CDCl_3$, δ (ppm), TMS ref] of BPTP100: 3.57-3.77 (C*H*$_2$-C*H*$_2$-O), 3.38 (C*H*$_3$-O), 2.55 (Si-CH$_2$-CH$_2$-C*H*$_2$-S-), 1.85 (Si-CH$_2$-C*H*$_2$-CH$_2$-S-), 0.62 (Si-C*H*$_2$-CH$_2$-CH$_2$-S-), 0.11 (Si-C*H*$_3$).

2.7.Cell fabrication and electrochemical characterization

Ionic conductivities of the SPEs were measured by complex impedance spectroscopy between 10 to 100 ^{o}C with a Zahner Electrik IM6 apparatus in the frequency range of 0.1 Hz to 1 MHz and an applied voltage of 10 mV. The real part of the impedance at the minimum of imaginary part was used as the resistance to calculate the conductivity of the SPEs. The samples for the measurements were prepared by sandwiching the SPEs between two stainless-steel electrodes. Each sample was allowed to equilibrate for 30 min at each temperature prior to taking the measurements. The ionic conductivity (σ) was calculated from the electrolyte resistance (R) obtained from the impedance spectrum, the electrolyte thickness (d) and the area of the electrode (A) using the equation, $\sigma = (1/R) \times (d/A)$. The electrochemical stability of the electrolytes was evaluated using linear sweep voltammetry (LSV). The cell was assembled by sandwiching electrolyte between stainless steel (working electrode) and lithium metal (reference electrode) in a 2032 coin cell. The cell was swept in the potential range from 3 V to 7 V (vs. Li/Li^{+}) at a

scan rate of 1 mV/s at 60 ^{o}C. Charge/discharge test of all-solid-state lithium-sulfur battery was performed with WBSC3000 battery cycler (WonATech) with cutoff voltages of 1.7 ~ 2.8 V (*vs*. Li/Li^{+}) at 60 ^{o}C. Elemental sulfur (60 wt%) was used as cathode active materials and dispersed in *N*-methyl-2-pyrrolidone with Super P (20 wt%) and PVDF (20 wt%). The cathode was coated with A-BPTP80 solution comprising BPT (0.05 g), LiTFSI (0.056 g, [Li]/[EO]=0.07), allyl PEO (0.13 g), allyl GA (0.007 g), and DMPA (0.005 g) dissolved in 0.2 mL of distilled THF via solution casting followed by fluorescent lamp irradiation for 16 h. The coated cathode was dried under high vacuum at 120 ^{o}C for 24 h prior to test. A-BPTP80 coated sulfur cathode and lithium metal anode were assembled together in a 2032 coin cell. In case of coin cell containing liquid electrolyte, Celgard 2320 was used as a separator and 1 M LiTFSI in DOE:DOL (1:1 vol%) with 0.1 M $LiNO_3$ was used as a liquid electrolyte instead of SPE. All components were assembled in argon filled glove box (H_2O < 0.5 ppm, O_2 < 0.5 ppm).

2.8.Characterization

^{1}H NMR spectra were recorded on an AscendTM 400 spectrometer (300 MHz) using $CDCl_3$ and $CDCl_3$ (Cambridge Isotope Laboratories) as a solvent at room temperature, with TMS as a reference. ^{29}Si NMR spectra were recorded on JeolJNM-LA400 spectrometer (400 MHz) using $CDCl_3$ (Cambridge Isotope Laboratories) as a solvent at room temperature. Molecular weights (M_n, M_w) and polydispersity index (PDI) were analyzed by gel permeation chromatography (GPC) equipped with a Waters 515 HPLC pump and three columns including PLgel 5.0 μm guard, MIXED-C, and MIXED-D from Polymer Laboratories. The refractive index (RI) detector was calibrated using polystyrene standards. The resulting data was analyzed using the Omnisec software. HPLC grade THF (J. T. Baker) was used as the eluent at a flow rate of 1.0 mL min^{-1} at 35 ^{o}C. The glass transition temperatures of the polymers were examined by differential scanning calorimetry (DSC) using TA Instruments DSC-Q1000 under a nitrogen atmosphere. Samples with a typical mass of 5.0-10 mg were encapsulated in sealed aluminum pans. The

samples were first heated to 150 ^{o}C and then quenched to -80 ^{o}C followed by a second heating scan from -80 ^{o}C to 150 ^{o}C at a heating rate of 10 ^{o}C min^{-1}. The thermal stability of the polymers was evaluated by thermogravimetric analysis (TGA) using TA Instruments TGA Q-5000IR under a nitrogen atmosphere. The samples were first heated to 130 ^{o}C for 10 minutes, and then heated to 700 ^{o}C at a heating rate of 10 ^{o}C min^{-1}. Temperature-resolved dynamic mechanical analysis (DMA) was conducted using a Q800 dynamic mechanical analyzer (TA Instruments) with 1 Hz of frequency at 10 ^{o}C/min ramp. Hot box (HB-37L, Canatech., Korea) was used to test long-term thermal stability of SPEs. The coin cells comprising sulfur cathode, electrolyte (1 M LiTFSI in DOE:DOL (1:1 vol%) with 0.1 M $LiNO_3$/Celgard 2320 or A-BPTPs), and lithium metal anode were placed in a hot-box and the temperature was increased from 25 ^{o}C to 150 ^{o}C by 2 ^{o}C/min. After the temperature reaches 150 ^{o}C, each cell was placed in a hot-box for long-term period. FT-IR spectra were recorded in the absorption mode on Nicolet 6700 spectrophotometer with a resolution of 4 cm^{-1} in the vibrational frequency range from 400 to 4000 cm^{-1}. Field-emission scanning electron microscopy (FE-SEM)

was performed on a JEOL JSM-6700F with an accelerating voltage of 10 kV.

3. Result and Discussion

3.1.Synthesis and preparation of components in SPEs

Scheme 3(a) shows the structure of solid-state polymer having ion-conducting PEO group crosslinked with allyl GA. Since polysiloxane has been known to very flexible due to its low barrier energy to bond rotation, polysiloxane was chosen as a polymer matrix for the SPE because flexible polymer chains with low glass transition temperature (T_g) conduct lithium ions well.[37] Branched polysiloxane having thiol group (BPT) was synthesized by acid-catalyzed hydrolysis and condensation reaction as shown in Scheme 2(a). The structure of BPT was confirmed by ^{1}H NMR and ^{29}Si NMR (Figure 1). After the reaction, protons in methoxy group of silane monomers at about 3.5 ppm clearly disappeared and protons in alkyl chains and thiol group appeared. The thiol groups provide a platform for further functionalization of the BPT through post-modification using thiol-ene click chemistry. As shown in ^{29}Si NMR spectrum, BPT has both D (-15.8

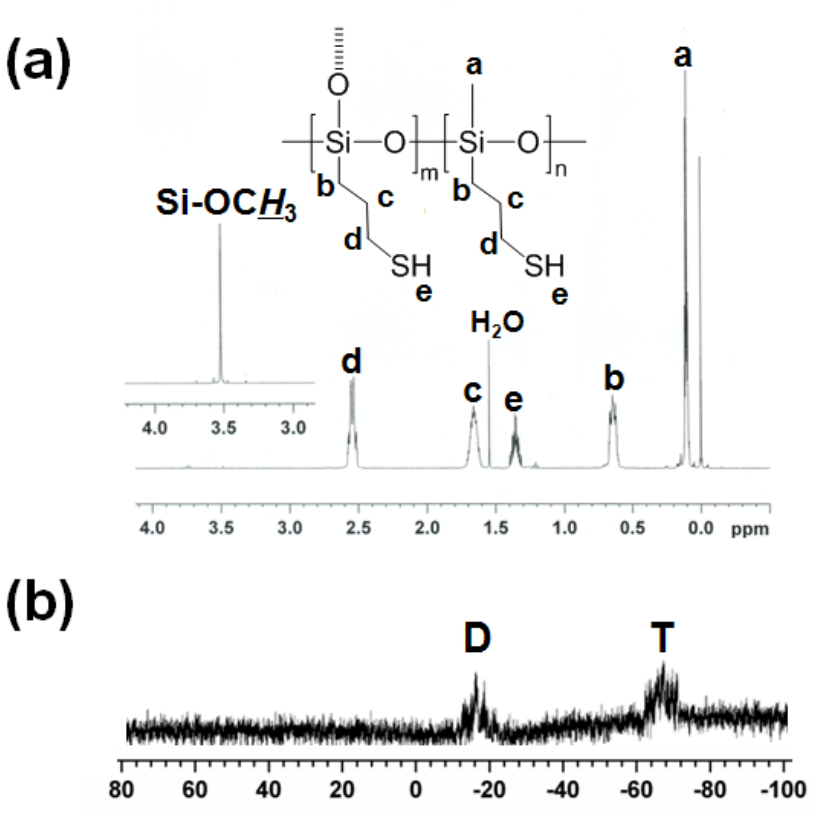

Figure 1 (a) ^{1}H NMR spectrum and (b) ^{29}Si NMR spectrum of BPT.

ppm) and T (-68.0 ppm) signal, indicating that BPT has a branched structure. To attach ion-conducting PEO and crosslinkable GA moieties to the thiol group of BPT, hydroxyl group of poly(ethylene glycol) methyl ether and phenol/carboxylic acid groups of GA were substituted by allyl group (Scheme 2(b) and 2(c)). The structures of allyl PEO and allyl GA were also confirmed by ^{1}H NMR. Figure 2 shows ^{1}H NMR spectra of allyl PEO and allyl GA, and it was found that proton peaks in allyl group of both allyl PEO and allyl GA were observed at 4.0~6.5 ppm, indicating that ally substitution was successfully conducted.

SPEs were prepared using simple one-pot curing process based on thiol-ene click reaction by irradiation of fluorescent lamp (Scheme 3(a)). Since the thiol-ene click reaction exhibits rapid reaction rate due to its click nature and high efficiency with low sensitivity to oxygen inhibition, irradiation of fluorescent lamp with low intensity was enough to induce the crosslinking reaction.[38] Furthermore, any expensive transition metal catalyst was not required compared to the case of typical Pt-catalyzed hydrosilylation reaction, indicating that the curing reaction used in SPE preparation is not energy-consuming process that does not require excessive

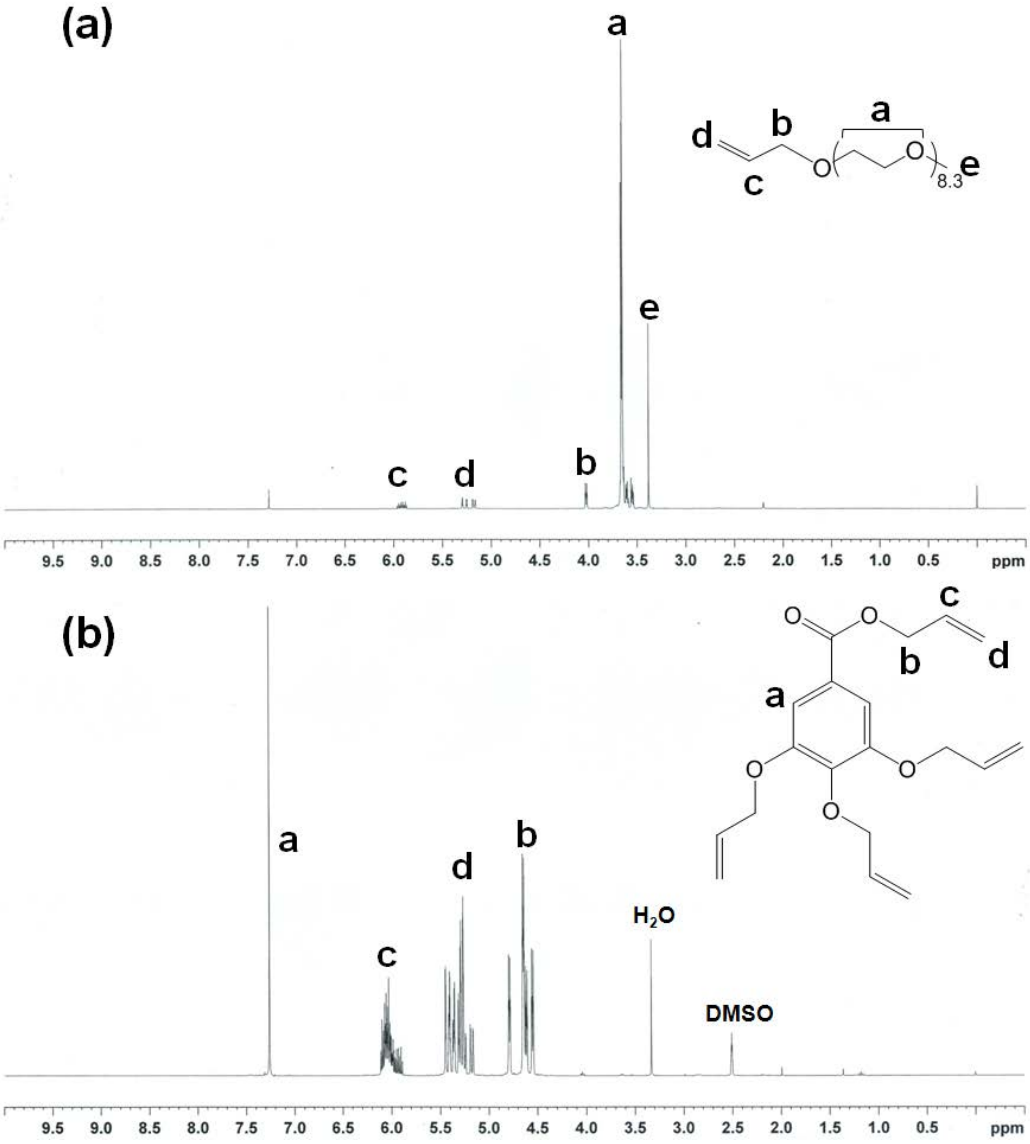

Figure 2 ^{1}H NMR spectra of (a) allyl PEO and (b) allyl GA.

power.

To study the effect of crosslinking density and ion-conduction PEO content, molar ratio of allyl PEO to allyl GA was varied as 50:50, 65: 35, and 80:20. For the convenience, SPEs having 50, 65, and 80 mol% of allyl PEO are abbreviated as A-BPTP50, A-BPTP65, and A-BPTP80, respectively. Polymer electrolyte having only the PEO group without allyl GA was also prepared, and it is abbreviated as BPTP100. As shown in Scheme 3(b), A-BPTP50, A-BPTP65, and A-BPTP80 were obtained as dimensionally-stable solid-state films, while the BPTP100 exhibited wax state, indicating that introduction of allyl GA as a crosslinker forms the solid-state. The crosslinked state of A-BPTPs was confirmed by FT-IR analysis (Figure 3). The thiol peak at about 2565 cm^{-1} of BPT clearly disappeared after the curing process from all the A-BPTPs, resulting in formation of fully crosslinked polymer network. Since the BPTP100 having a wax state is easily soluble in common organic solvent, ^{1}H NMR and GPC analysis was conducted. Figure 4 shows ^{1}H NMR spectrum of BPTP100. The protons in thiol group of BPT and allyl group of

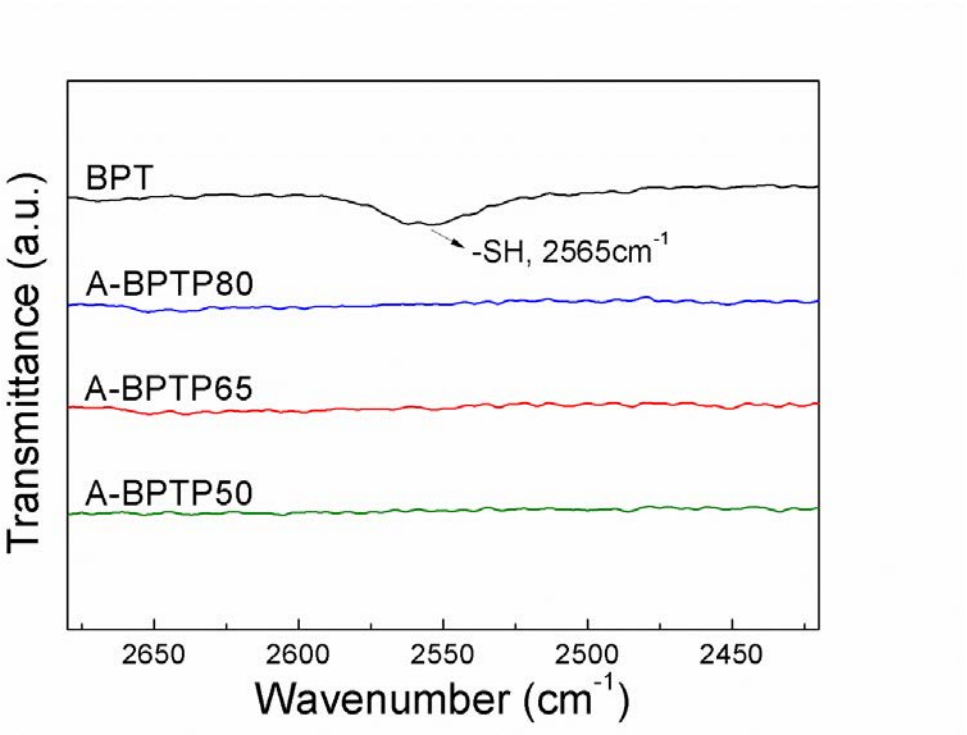

Figure 3 FT-IR spectra of BPT and A-BPTPs, where the number in the abbreviation indicates mol% of PEO groups.

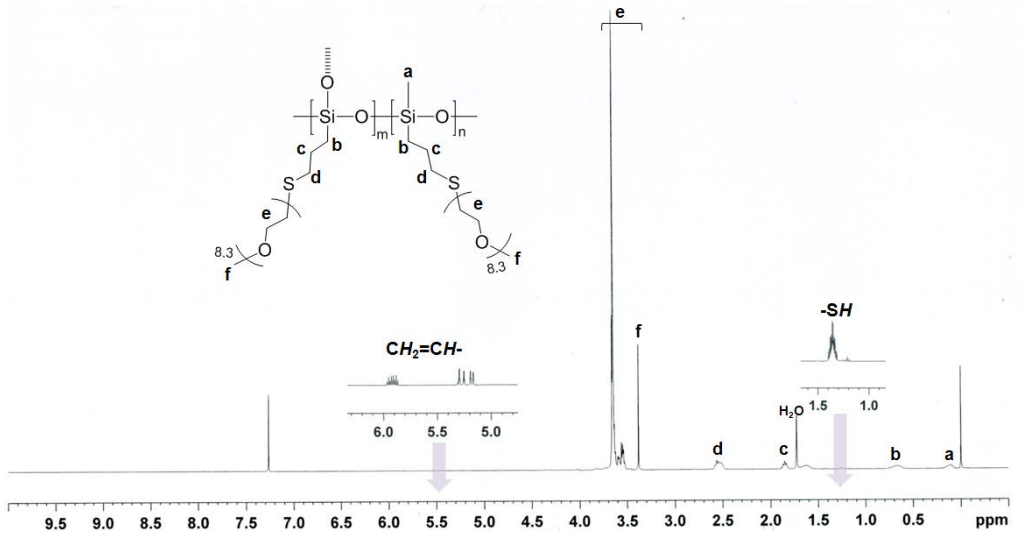

Figure 4 ^{1}H NMR spectrum of BPTP100.

allyl PEO disappeared after the thiol-ene click reaction, and protons assigned to PEO group appeared at 3.3~3.8 ppm. Furthermore, the molecular weight of BPTP100 was found to be higher than that of BPT due to the PEO grafting as shown in GPC profiles (Figure 5).

Figure 6 shows surface SEM images of A-BPTPs. There are no pores and wrinkles on the surface of A-BPTPs, while the pores and wrinkles are commonly observed from the crosslinked polymer network due to macroscopic phase separation originated from immiscibility between monomers and crosslinkers.[26] In contrast, A-BPTPs did not show such behaviors, indicating that all the components are homogeneously embedded in the crosslinked polymer network.[39] The pore-free surface of the SPEs can suppress physical penetration of lithium polysulfides and lithium dendrites occurred in lithium-sulfur batteries as will be described in the later part of this paper.

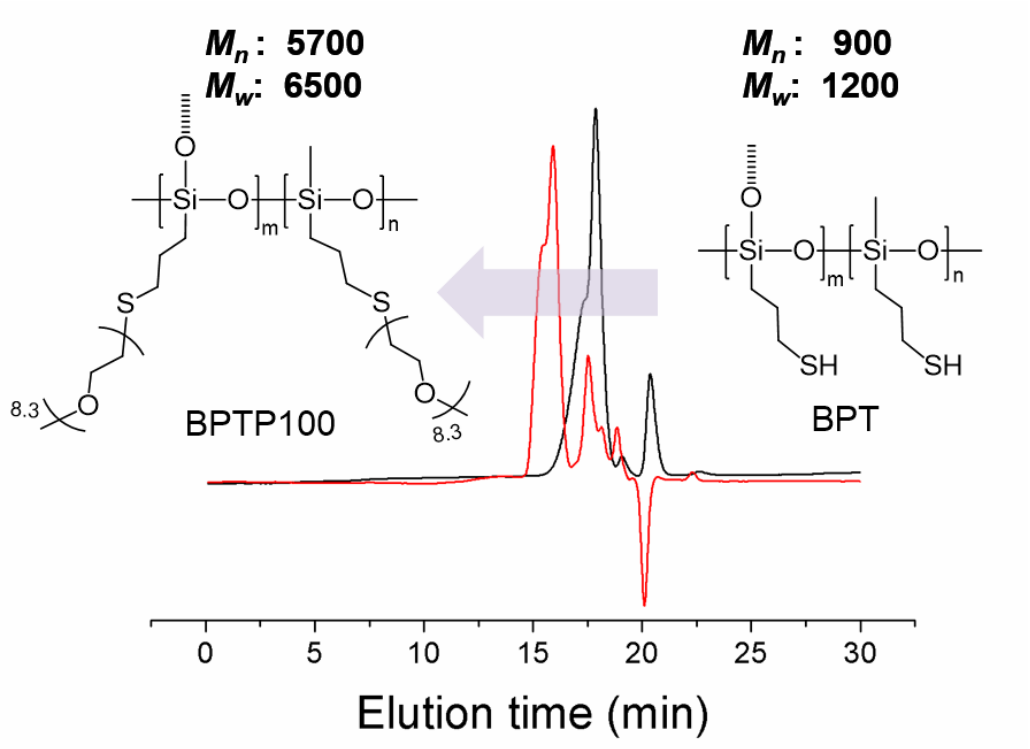

Figure 5 GPC profile of BPT and BPTP100.

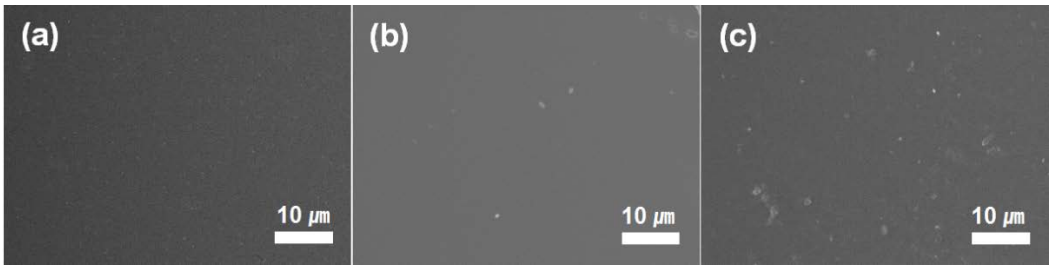

Figure 6 Surface SEM images of (a) A-BPTP50, (b) A-BPTP65, and (c) A-BPTP80 (scale bar: 10 μm).

3.2.Thermal, mechanical, and electrochemical stabilities

Figure 7(a) shows TGA profiles of A-BPTPs. It was found that thermal decomposition of A-BPTPs was not observed up to nearby 300 ^{o}C, implying that A-BPTPs can be used for high-temperature battery applications such as electric vehicles and energy storage system. The decomposition temperature at 5 wt% of weight loss ($T_{d,5\%}$) values of A-BPTP50, A-BPTP65, and A-BPTP80 are found to 294 ^{o}C, 288 ^{o}C, and 294 ^{o}C, respectively. The char yield at 700 ^{o}C increases as the allyl GA content increase (or allyl PEO content decrease) because the weight percent of polysiloxane, BPT, increases in the crosslinked polymer network. Since the residual weight at 700 ^{o}C in TGA profiles is attributed to the silicon oxide from the siloxane backbone of BPT, the char yield is dependent on the BPT content. Dynamic mechanical analysis (DMA) was also conducted to show the thermomechanical property of A-BPTPs. Figure 7(b) shows temperature dependence of storage modulus (E') behaviors of A-BPTPs. It was found that storage modulus values of A-BPTPs are maintained well as the temperature

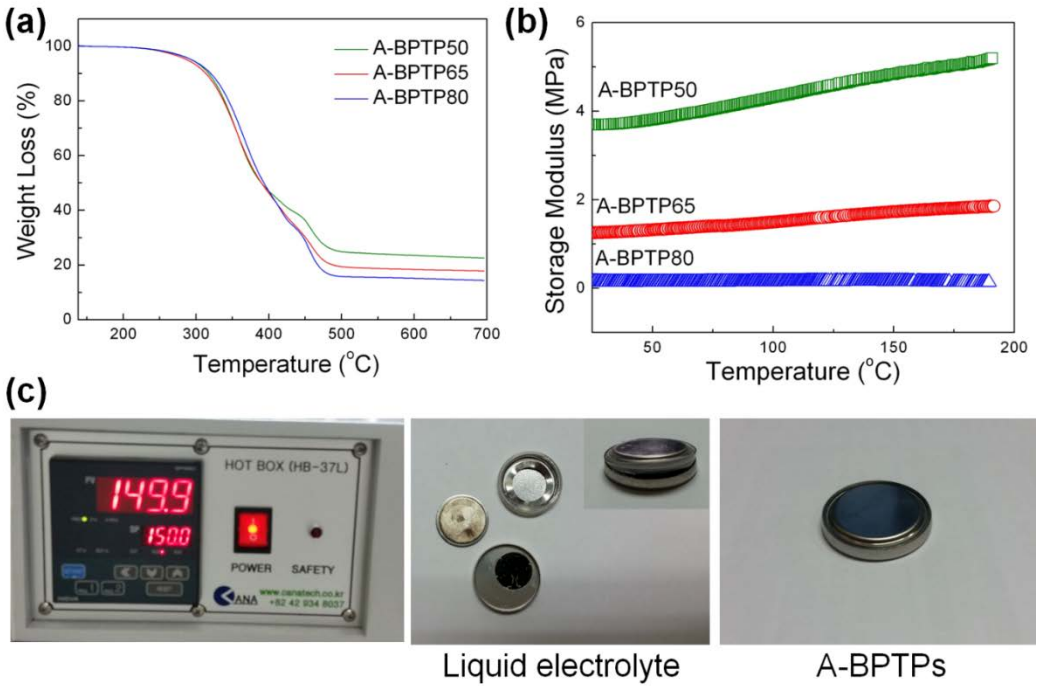

Figure 7 (a) TGA profiles of A-BPTPs, (b) temperature-resolved DMA behaviors of A-BPTPs, and (c) hot-box test of coin cells containing liquid electrolyte and A-BPTPs.

increases up to 200 ^{o}C because allyl GA having four crosslinkable allyl groups forms very stable crosslinked polymer network.[31, 33] Furthermore, the E' value of the A-BPTPs was found to increase as the allyl GA content increases because crosslinking density of the polymer increases.[33]

Comparing to the commonly used liquid electrolytes, A-BPTPs showed long-term thermal stability at 150 ^{o}C as shown in Figure 7(c). The coin cells comprising sulfur cathode, electrolyte (liquid electrolyte/separator or A-BPTPs), and lithium metal anode were placed in a hot-box and the temperature was increased from 25 ^{o}C to 150 ^{o}C by 2 ^{o}C/min. After the temperature reaches 150 ^{o}C, each cell was placed in a hot-box for long-term period. The coin cell containing liquid electrolyte was exploded after 15 min as shown in the inset photograph of Figure 7(c). Furthermore, organic solvents in the liquid electrolyte were evaporated in the hot-box and Celgard separator also shrunk. Since the most liquid electrolytes have high volatility and flammability, operation of the cells containing liquid electrolytes might cause thermal runaway of battery system.[40] In contrast, the coin cells containing A-BPTPs maintain their pristine state without any swelling or explosion

at 150 ^{o}C, indicating that crosslinked SPE with excellent thermal stability should be used for the high-temperature battery applications.

3.3.Ion conduction property

Figure 8(a) shows temperature dependence of ionic conductivities of BPTP100 and A-BPTPs. BPTP100 having a wax state exhibits higher ionic conductivity than those of A-BPTPs having solid-states, because segmental mobility of ion-conduction PEO group is higher in the waxy polymer matrix than in the solid-state film.[20] As shown in DSC thermograms in Figure 8(b), glass transition temperature (T_g) value of BPTP100 is lower than those of A-BPTPs.

Ionic conductivities of A-BPTPs increase with the increase of PEO content as expected from the DSC results; The T_g values of A-BPTP50, A-BPTP65, and A-BPTP80 are -50.3 ^{o}C, -46.8 ^{o}C, and -45.5 ^{o}C, respectively. Since the crosslinking density decreases as the PEO content increases, chain mobility of PEO group of A-BPTP80 is highest among the series of A-BPTPs, resulting in highest ionic conductivity.[26] The ionic conductivities of A-BPTP80 are even comparable to those of BPTP100 having a wax state, indicating that the chain mobility of PEO group is preserved well even in the crosslinked polymer network. For example, ionic

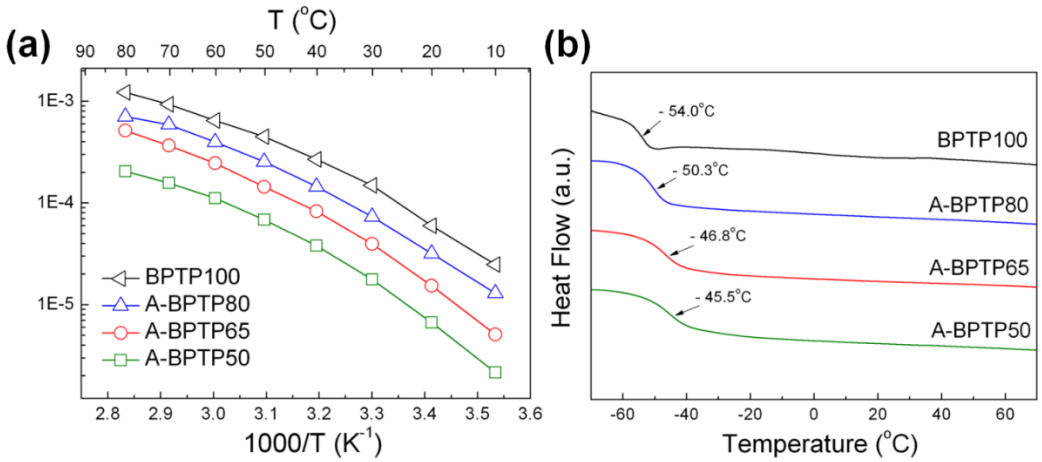

Figure 8 (a) Temperature dependence of ionic conductivities of BPTP100 and A-BPTPs, where each electrolyte contains same LiTFSI concentration ([Li]/[EO]=0.07) and (b) DSC thermograms of BPTP100 and A-BPTPs.

conductivity values of A-BPTP80 and BPTP100 at 60 ºC are 4.0×10^{-4} S/cm and 6.5×10^{-4} S/cm, respectively. It is noteworthy that A-BPTP80 exhibits sufficient mechanical stability as a solid-state free-standing film as well as high ionic conductivity comparable to waxy BPTP100.

3.4.Electrochemical and interfacial compatibility with electrodes

The electrochemical stability of A-BPTP80 was evaluated using linear sweep voltammetry (LSV) (Figure 9). It was found that electrochemical oxidative decomposition was not occurred until the voltage reaches 5.4 V (*vs*. Li/Li^+), indicating that there might be no electrochemical decomposition within the operation voltage range of sulfur cathode, 1.7~2.8 V. Furthermore, A-BPTP80 is also compatible with other 4 V class cathode materials such as $LiCoO_2$, LiV_3O_8, and $LiFePO_4$.

Interfacial compatibility of A-BPTP80 with lithium metal anode was evaluated by measuring the time dependence of interfacial resistances of symmetric lithium cells for 30 days (Figure 10). Since the highly reactive lithium metal easily reacts with almost all the chemical species in the electrolytes including small amount of oxygen and residual solvents, unstable and inhomogeneous solid electrolyte interphase (SEI) layer is inevitably formed at the interfaces between electrolyte and lithium metal anode, resulting in increase of interfacial resistance.[41] Although the SEI layer can

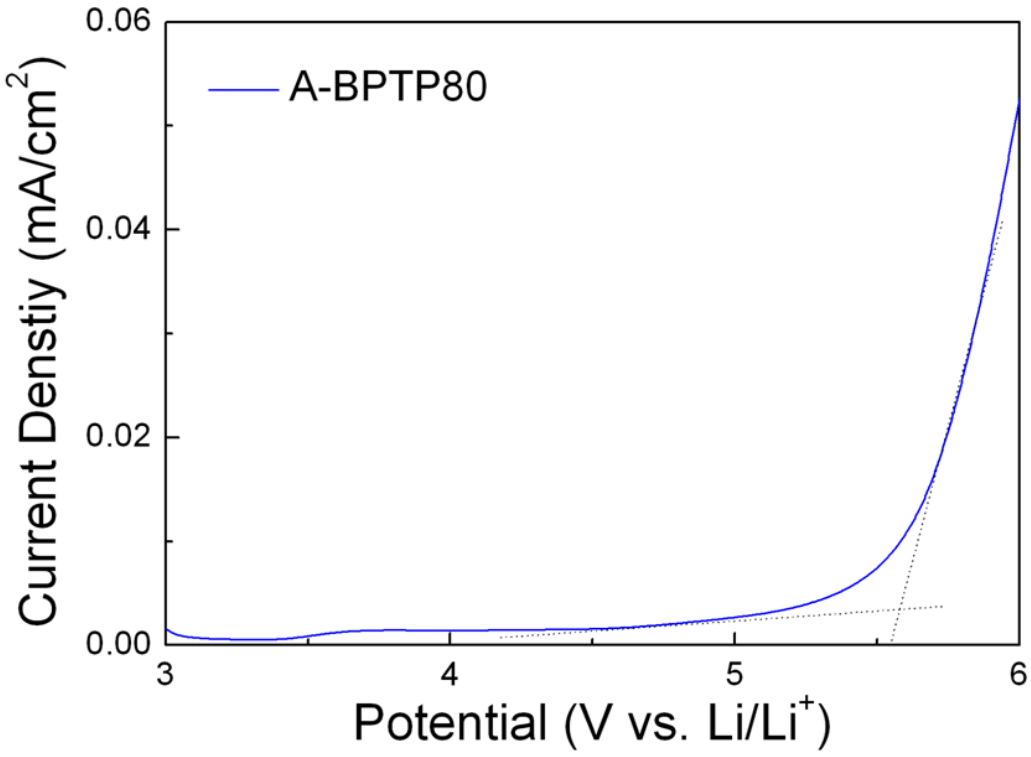

Figure 9 Linear sweep voltammogram A-BPTP80 at 60 ^{o}C with a scan rate of 1 mV/s.

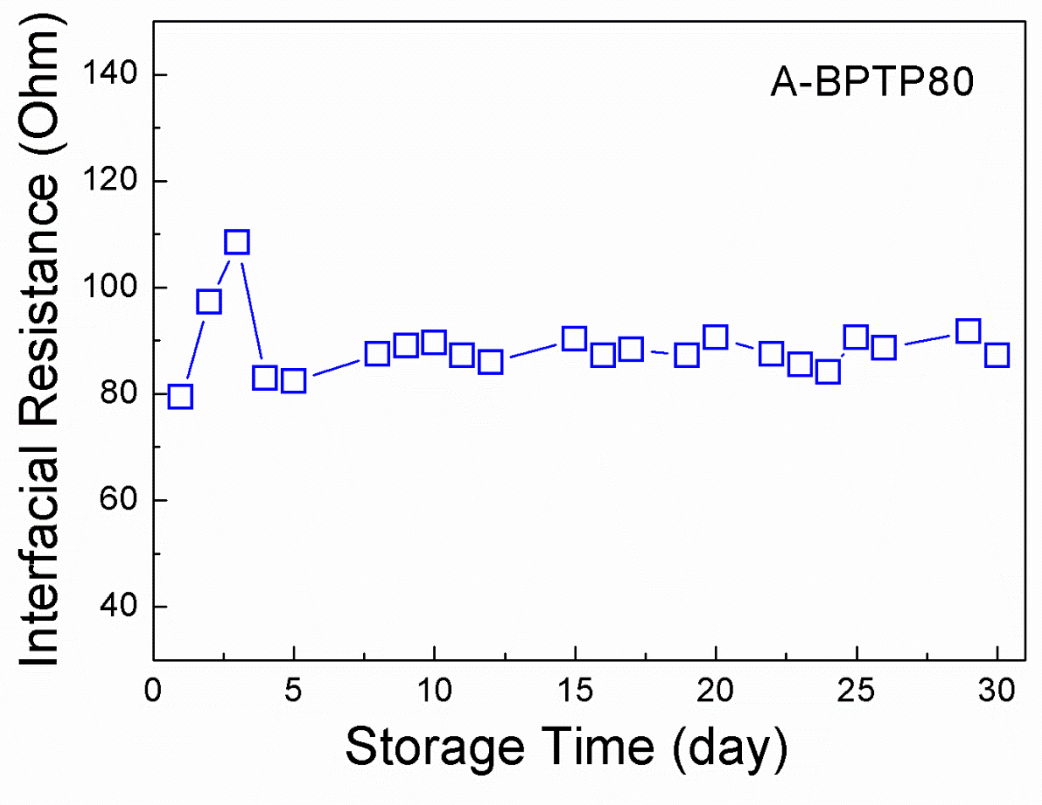

Figure 10 Interfacial resistances of symmetric lithium cell containing A-BPTP80 stored under open-circuit condition at 60 ^{o}C as a function of storage time.

act as a protective barrier against further possible side reactions between lithium and other impurities, formation of SEI layer having irregular structure accelerates lithium dendrite growth and also increases the overall resistances against efficient charge transport.[42] As shown in Figure 10, interfacial resistances of the cell containing A-BPTP80 slightly increase with the storage time at first and then maintain almost constant values for 30 days. Because the solvent-free and solid-state A-BPTP80 excludes the possibility of violent side reactions commonly occurred in conventional liquid electrolyte cell, our solid-state system significantly reduces the those kinds of side reactions and also contributes to form stable SEI layer.[43, 44]

3.5.Preparation of all-solid-state lithium-sulfur battery

All-solid-state lithium-sulfur battery was fabricated using direct solution casting of A-BPTP80 on a sulfur cathode as illustrated in Scheme 4. Since the sulfur cathode comprising sulfur, Super P, and PVDF binder has a porous structure, solid-state A-BPTP80 cannot penetrate into the pores when the sulfur cathode and A-BPTP80 are just sandwiched in a coin cell which increases the interfacial resistance. The porous sulfur cathode can be filled by A-BPTP80 by direct solution casting of A-BPTP80 on a sulfur cathode followed by irradiation of fluorescent lamp. After assembling with lithium metal anode, all-solid-state lithium-sulfur battery can be fabricated. This integrated cathode-electrolyte system can further decrease the problematic dissolution of lithium polysulfides because the polysulfides cannot be dissolved in solid-state A-BPTP80, while such dissolution is easily occurred in the battery containing liquid electrolyte (Scheme 5). Furthermore, solid-state A-BPTP80 filled in the porous sulfur cathode can interact with lithium polysulfides by some interaction, thereby suppressing mitigation of lithium polysulfide toward the lithium metal anode.

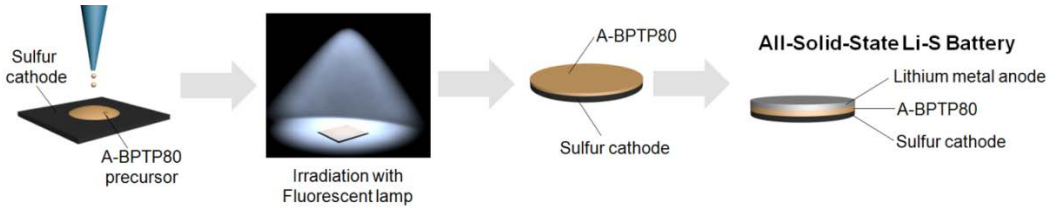

Scheme 4 Schematic illustration of fabrication of all-solid-state lithium-sulfur battery.

-

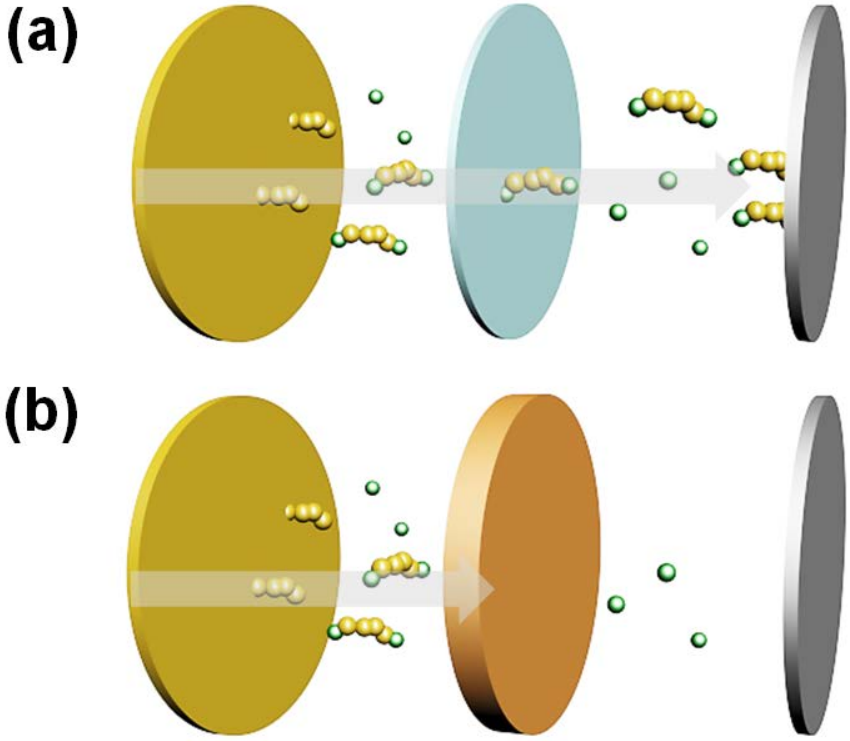

Scheme 5 Polysulfides dissolution behaviors of the battery containing (a) liquid electrolyte/separator and (b) SPE.

4. Conclusions

All-solid-state lithium-sulfur batteries were prepared using SPE based on crosslinked polysiloxane having ion-conducting PEO group and allyl-substituted natural phenolic acid, gallic acid. SPEs were prepared by facile one-pot curing process with fluorescent lamp irradiation via highly efficient thiol-ene click reaction. Good thermal and mechanical stabilities of SPEs are attributed to formation of stable crosslinked polymer network based on gallic acid crosslinker having four allyl groups. A-BPTP80 showed high ionic conductivity of 4.0×10^{-4} S/cm at 60 ^{o}C that is even comparable to that of waxy BPTP100 due to well-designed flexible polymer structure. All-solid-state lithium-sulfur battery was fabricated by using electrolyte-electrode integrated system to decrease large interfacial resistance between SPE and sulfur cathode as well as suppress the dissolution of lithium polysulfides. The all-solid-state lithium sulfur battery system is expected to exhibit excellent cycle performance and polysulfides-trapping effect of SPE will be investigated by XPS, EDX mapping, and density functional theory (DFT) studies.

5. References

1. Q. Pang, X. Liang, C. Y. Kwok and L. F. Nazar, *Nature Energy*, 2016, **1**, 16132.
2. P. G. Bruce, S. A. Freunberger, L. J. Hardwick and J.-M. Tarascon, *Nat Mater*, 2012, **11**, 19-29.
3. Y. X. Yin, S. Xin, Y. G. Guo and L. J. Wan, *Angewandte Chemie-International Edition*, 2013, **52**, 13186-13200.
4. Z. W. Seh, Y. M. Sun, Q. F. Zhang and Y. Cui, *Chem Soc Rev*, 2016, **45**, 5605-5634.
5. G. Zheng, Y. Yang, J. J. Cha, S. S. Hong and Y. Cui, *Nano Letters*, 2011, **11**, 4462-4467.
6. M.-Q. Zhao, Q. Zhang, J.-Q. Huang, G.-L. Tian, J.-Q. Nie, H.-J. Peng and F. Wei, *Nat Commun*, 2014, **5**, 3410.
7. X. Ji, K. T. Lee and L. F. Nazar, *Nat Mater*, 2009, **8**, 500-506.
8. L. Ji, M. Rao, H. Zheng, L. Zhang, Y. Li, W. Duan, J. Guo, E. J. Cairns and Y. Zhang, *J Am Chem Soc*, 2011, **133**, 18522-18525.
9. L. F. Xiao, Y. L. Cao, J. Xiao, B. Schwenzer, M. H. Engelhard, L. V. Saraf, Z. M. Nie, G. J. Exarhos and J. Liu, *Advanced Materials*, 2012, **24**, 1176-1181.
10. J. Wang, J. Chen, K. Konstantinov, L. Zhao, S. H. Ng, G. X. Wang, Z. P. Guo and H. K. Liu, *Electrochim Acta*, 2006, **51**, 4634-4638.
11. W. Li, Q. Zhang, G. Zheng, Z. W. Seh, H. Yao and Y. Cui, *Nano Letters*, 2013, **13**, 5534-5540.
12. G. Ma, F. Huang, Z. Wen, Q. Wang, X. Hong, J. Jin and X. Wu, *Journal of Materials Chemistry A*, 2016, **4**, 16968-16974.
13. C. Y. Li, A. L. Ward, S. E. Doris, T. A. Pascal, D. Prendergast and B. A. Helms, *Nano Letters*, 2015, **15**, 5724-5729.
14. S. Bai, K. Zhu, S. Wu, Y. Wang, J. Yi, M. Ishida and H. Zhou, *Journal of Materials Chemistry A*, 2016, **4**, 16812-16817.
15. J. Yoo, S. J. Cho, G. Y. Jung, S. H. Kim, K. H. Choi, J. H. Kim, C. K. Lee, S. K. Kwak and S. Y. Lee, *Nano Letters*, 2016, **16**, 3292-3300.
16. A. Varzi, R. Raccichini, S. Passerini and B. Scrosati, *Journal of Materials Chemistry A*, 2016, **4**, 17251-17259.
17. D. Zhou, R. L. Liu, Y. B. He, F. Y. Li, M. Liu, B. H. Li, Q. H. Yang, Q. Cai and F. Y.

Kang, *Adv Energy Mater*, 2016, **6**.
18. R. Khurana, J. L. Schaefer, L. A. Archer and G. W. Coates, *J Am Chem Soc*, 2014, **136**, 7395-7402.
19. V. Etacheri, R. Marom, R. Elazari, G. Salitra and D. Aurbach, *Energ Environ Sci*, 2011, **4**, 3243-3262.
20. J. Shim, D.-G. Kim, J. H. Lee, J. H. Baik and J.-C. Lee, *Polymer Chemistry*, 2014, **5**, 3432-3442.
21. S. K. Kim, D. G. Kim, A. Lee, H. S. Sohn, J. J. Wie, N. A. Nguyen, M. E. Mackay and J. C. Lee, *Macromolecules*, 2012, **45**, 9347-9356.
22. D. G. Kim, H. S. Sohn, S. K. Kim, A. Lee and J. C. Lee, *J Polym Sci Pol Chem*, 2012, **50**, 3618-3627.
23. D. G. Kim, J. M. Shim, J. H. Lee, S. J. Kwon, J. H. Baik and J. C. Lee, *Polymer*, 2013, **54**, 5812-5820.
24. J. Shim, D. G. Kim, H. J. Kim, J. H. Lee and J. C. Lee, *Acs Appl Mater Inter*, 2015, **7**, 7690-7701.
25. J. Shim, D. G. Kim, H. J. Kim, J. H. Lee, J. H. Baik and J. C. Lee, *Journal of Materials Chemistry A*, 2014, **2**, 13873-13883.
26. J. Shim, K. Y. Bae, H. J. Kim, J. H. Lee, D. G. Kim, W. Y. Yoon and J. C. Lee, *Chemsuschem*, 2015, **8**, 4133-4138.
27. S. J. Kwon, D. G. Kim, J. Shim, J. H. Lee, J. H. Baik and J. C. Lee, *Polymer*, 2014, **55**, 2799-2808.
28. J.-H. Baik, D.-G. Kim, J. Shim, J. H. Lee, Y.-S. Choi and J.-C. Lee, *Polymer*, 2016, **99**, 704-712.
29. R. Liu, J. Zhu, J. Luo and X. Liu, *Progress in Organic Coatings*, 2014, **77**, 30-37.
30. S. Q. Ma, Y. H. Jiang, X. Q. Liu, L. B. Fan and J. Zhu, *Rsc Adv*, 2014, **4**, 23036-23042.
31. C. Aouf, H. Nouailhas, M. Fache, S. Caillol, B. Boutevin and H. Fulcrand, *Eur Polym J*, 2013, **49**, 1185-1195.
32. J. Qin, H. Liu, P. Zhang, M. Wolcott and J. Zhang, *Polym Int*, 2014, **63**, 760-765.
33. G. Z. Yang, S. L. Kristufek, L. A. Link, K. L. Wooley and M. L. Robertson, *Macromolecules*, 2015, **48**, 8418-8427.
34. C. Aouf, C. Le Guernevé, S. Caillol and H. Fulcrand, *Tetrahedron*, 2013, **69**, 1345-

1353.
35. B. Badhani, N. Sharma and R. Kakkar, *Rsc Adv*, 2015, **5**, 27540-27557.
36. A. P. Subramanian, A. A. John, M. V. Vellayappan, A. Balaji, S. K. Jaganathan, E. Supriyanto and M. Yusof, *Rsc Adv*, 2015, **5**, 35608-35621.
37. Y. Kang, W. Lee, D. Hack Suh and C. Lee, *J Power Sources*, 2003, **119–121**, 448-453.
38. C. E. Hoyle and C. N. Bowman, *Angewandte Chemie-International Edition*, 2010, **49**, 1540-1573.
39. Y. J. Zuo, J. F. Cao and S. Y. Feng, *Advanced functional materials*, 2015, **25**, 2754-2762.
40. T. M. Bandhauer, S. Garimella and T. F. Fuller, *J Electrochem Soc*, 2011, **158**, R1-R25.
41. W. Xu, J. L. Wang, F. Ding, X. L. Chen, E. Nasybutin, Y. H. Zhang and J. G. Zhang, *Energ Environ Sci*, 2014, **7**, 513-537.
42. X. B. Cheng, R. Zhang, C. Z. Zhao, F. Wei, J. G. Zhang and Q. Zhang, *Adv Sci*, 2016, **3**.
43. C. Xu, B. Sun, T. Gustafsson, K. Edstrom, D. Brandell and M. Hahlin, *Journal of Materials Chemistry A*, 2014, **2**, 7256-7264.
44. P. Hu, Y. Duan, D. Hu, B. Qin, J. Zhang, Q. Wang, Z. Liu, G. Cui and L. Chen, *Acs Appl Mater Inter*, 2015, **7**, 4720-4727.

국문 요약

자연 유래 물질인 갈릭산을 이용하여 가교제를 합성하고, 싸이올-엔 클릭 반응을 통해 이온전도성 PEO 그룹을 포함하는, 폴리실록산 기반 가교 구조의 고체상 고분자 전해질을 제조하였다. 가교 밀도 및 PEO 함량이 전해질 성능에 미치는 효과를 분석하기 위해 일련의 전해질들을 제조한 결과, 모든 전해질들이 치수안정성이 좋은 자유지지형 필름의 형태로 얻어졌으며 안정한 가교 구조로 인해 우수한 열적, 기계적 및 전기화학적 안정성을 나타내었다. 특히 PEO 그룹 및 갈릭산 가교제 함량이 각각 80 mol%, 20 mol% 인 전해질의 경우, 가교 구조를 갖지 않는 왁스형 전해질에 버금가는 높은 이온 전도도 (4.0×10^{-4} S/cm at 60 ºC) 를 보였다. 이처럼 자연 유래 갈릭산 유도체로 가교된 고체상 고분자 전해질은 안전한 고온용 배터리 시스템에 적용 가능할 것으로 기대되며 나아가 전고체형 리튬-황전지로의 응용도 기대해 볼 수 있다.

주요어: 리튬-황 전지, 전고체 리튬 금속 전지, 고체상 고분자 전해질, 갈릭산, 싸이올-엔 클릭 반응

학번: 2015-21041